A Network Science Cartography of Cognitive Control System Dynamics

Carrisa V Cocuzza (carrisacocuzza@gmail.com)[1]
Julia Hamilton (julialindsayhamilton@gmail.com)[1]
Emily Winfield (emwinfield4@gmail.com)[1]
Danielle S. Bassett (dsb@seas.upenn.edu)[2]
Michael W Cole (mwcole@gmail.com)[1]
[1]Center for Molecular and Behavioral Neuroscience, Rutgers, 197 University Avenue Newark, NJ 07102 United Sates
[2]Departments of Bioengineering, Physics & Astronomy, Electrical & Systems Engineering, and Neurology, University of Pennsylvania, 210 S. 33rd Street, Philadelphia, PA 19104 United States

Abstract

Functional connectivity studies have identified at least two large-scale neural systems that constitute cognitive control networks (CCNs) – the frontoparietal (FPN) and cingulo-opercular (CON) networks. CCNs are thought to support goal-directed cognition and behavior. We previously showed that FPN shifts global connectivity by task goal, consistent with a "flexible hub" mechanism for cognitive control. Our aim here is to develop a functional cartography of CCNs in terms of network mechanisms. We quantified mechanisms using a high-demand control paradigm involving switching among 64 systematically-related tasks. We hypothesized that cognitive control is enacted differently by the FPN and CON, and found dissociations in graph metric results across these networks. Consistent with a flexible hub mechanism, FPN connections were globally diverse, while tending to maintain their within-network connectivity across tasks. Consistent with a "stable hub" mechanism, CON connections were globally uniform (consistently connecting to the same networks), while tending to not maintain within-network connections. This pattern of results suggests FPN acts as a dynamic, global coordinator of goal-relevant information, while CON transiently disbands to dynamically lend resources to other goal-relevant networks. This cartography of network dynamics reveals a dissociation between two prominent cognitive control networks, suggesting parallel distinct mechanisms underlying goal-directed cognition.

Keywords: cognitive control; network dynamics; graph theory

Cognitive Control

Control theory (a core framework in engineering) suggests that flexibly reconfigurable systems are well-suited for control processing (Cao et al., 2012). In neural systems, we propose this function is borne out as *cognitive control*, or processes supporting goal-directed cognition (Egner, 2017). An individual's goals, the environment, and the state of the system are all subject to change over time. To accord with these fluctuations, control processing must be dynamic (Miller & Cohen, 2001). Here we asked how control is instantiated in terms of the spatiotemporal dynamics driving brain network reconfiguration. We aimed to develop functional cartographies representing pivotal network properties in two dimensions. Cartographies act as "maps" for network mechanisms or properties of interest (Guimerà et al., 2005; Mattar et al., 2015). Understanding the neural basis of cognitive control has broad implications, including potential applications in mental health, education, better goal-pursuit strategies for everyday life, and improved artificial intelligence for *in silico* modeling of neural networks.

Cognitive control networks (CCNs) are posited to include at least two large-scale systems – the frontoparietal (FPN) and cingulo-opercular (CON) networks (Dosenbach et al., 2008). The FPN is thought to contain *flexible hub regions* – or network nodes with extensive connectivity (hubs) that are capable of rapid reconfiguration with changing task demands (flexible) (Cole et al., 2013b). Outstanding questions remain regarding the CON: does it also contain hub-like regions? Are they likewise flexible?

Intrinsic and Task-Evoked Systems

Cognitive control is thought to be exhibited based on current task-demands and the current capability of the system (Miller & Cohen, 2001). Two important findings informed our thinking regarding cognitive control for the current study. (1) Task-evoked functional connectivity (tFC) across many states closely resembles intrinsic, resting-state connectivity (rsFC) (Cole et al., 2014). Moreover, slight changes from rsFC to tFC carry functional properties supporting the task at hand (Hearne et al., 2017). (2) The amount of control deployed reduces with expertise; the more practiced one is at a given task, the less they utilize control (Schnieder & Chein, 2002).

To investigate *ongoing* control processing, we administered a rapid instructed task learning (RITL) cognitive paradigm – the concrete permuted rule operations (C-PRO) paradigm (Cole et al., 2013a; Ito et al., 2017) – during functional magnetic resonance imaging (fMRI). This paradigm combined sensory, motor, and logic rules such that each task state presented a novel permutation to the participants. Cognitive control was required across all trials per the

presentation of novel combinations of complex rule sets. Resting-state fMRI scans were also obtained, allowing us to synthesize the benefits of a RITL paradigm with the observation that task-evoked states emerge out of an intrinsic state (**Fig. 1**), and assess functional reconfigurations between these states (**Fig. 2 & 3**). The cohort included N=100 healthy adults (44 men and 56 women, mean age of 22 years, SD=4.05 years); all of which provided informed consent. To improve replicability, we used a split-sample validation approach with an n=50 'discovery' dataset and an n=50 'replication' dataset (discovery data shown herein).

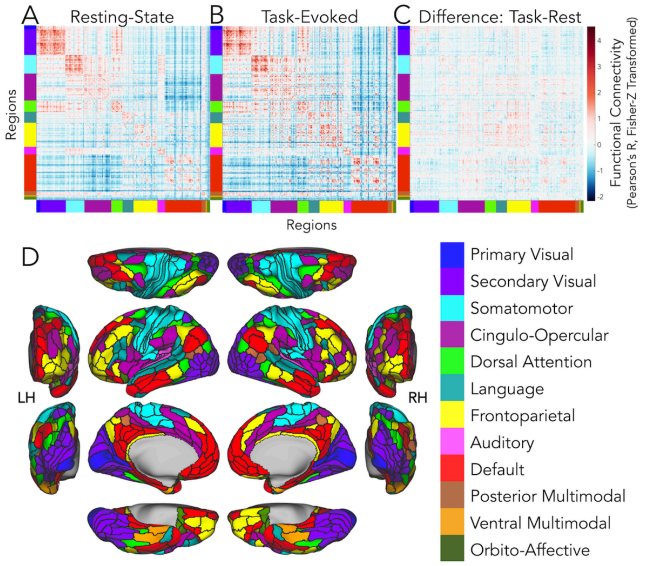

Figure 1: **Functional connectivity (FC) estimation. (A)** Resting-state functional connectivity (rsFC) across 360x360 regions (parcellation as in Glasser et al., 2016), ordered per the CA partition (color-coded along each matrix edge; see D). Values are discovery-set grand averages (n=50, 15-minute duration). rsFC was estimated with Pearson's correlation coefficient, Fisher z-transformed for stabilization of variance**. (B)** Task-evoked functional connectivity (tFC) across 360x360 brain regions, ordered and estimated as in A (grand averages: n=50 and 64 C-PRO task states). **(C)** Difference matrix: tFC-rsFC. Two-dimensional correlation coefficient between tFC (B) and rsFC (A), R=0.88, p<0.00001 (r^2~78% shared variance explained). **(D)** Cortical schematic of the Cole-Anticevic (CA) intrinsic network partition (Spronk et al., 2018). LH = left hemisphere; RH = right hemisphere.

Network Dynamics Metrics

To quantify mechanisms underlying changes in FC across C-PRO task states, we employed graph theoretical metrics previously developed to characterize network dynamics. In some cases, they have already been linked with the flexible reconfiguration property of control processing. This network mechanism approach is thought to provide explanatory power to observed links between neural data and cognitive demands (as well as behavioral output) (Mill et al., 2017). Importantly, graph metrics quantifying network dynamics can vary on mathematical assumptions, data treatment, and null-model comparison, but are often interpreted similarly. We probed these metrics by comparing results with algorithmic properties in mind, to ultimately build a mechanistically detailed cartography of CCNs.

Global Variability Coefficient (GVC)

Global variability coefficient (GVC) quantifies shifting patterns of tFC across states. GVC is calculated based on the standard deviation of each connection across task states, which are then averaged across all connections for each region. Networks with high GVC contain flexible hub regions capable of exerting adaptive task control (Cole et al., 2013). Confirming previous findings, we found the FPN had the highest GVC, t(49)=11.83, p<<0.01. (**Fig. 2A & 2B**). GVC treats data as derived from a continuous distribution.

Between-Network Variability Coefficient (BVC)

Between-network variability coefficient (BVC) is a version of GVC wherein within-network connections are withheld from computations. This measure accounts for the potential confound that within-network tFC estimates might confer upon GVC results (if one is interested primarily in global, out-of-network dynamics). We found that BVC was tightly correlated with GVC results ($r_s(10)=0.96$, p<<0.01), suggesting that within-network estimates do not dominate the outcome of the GVC analysis. FPN regions likewise demonstrated the highest BVC; t(49)=12.36, p<<0.01 (**Fig. 2C & 2D**). This pattern of results supports the notion that the FPN contains flexible regions adaptively configured for multi-task control.

Network Flexibility (NF)

Network flexibility (NF) measures spatiotemporal dynamics related to task-evoked time-series by quantifying temporal variability in network organization (Bassett et al., 2011; Bassett et al., 2013). This organization was identified by an optimized quality function termed multilayer modularity (Mucha et al., 2010). Required parameters (γ,ω) could be used to tune the degree to which connectivity dynamics were treated as discrete versus continuous in space (γ) and/or time (ω). This tuning ultimately determined whether NF was correlated or uncorrelated with GVC. We varied γ between 0 and 5 in steps of 0.5; ω, between 0 and 2 in steps of 0.2. NF was strongly correlated with GVC when γ=3 and ω=0.2, which we termed NF-optimal ($r_s(10)=0.8$, p=0.0032). NF was uncorrelated with GVC in the field-standard portion of the parameter space, or when γ=1 and ω=1

($r_s(10)=0.21$, p=0.51) (Chen et al. 2015), which we termed NF-standard. We propose that NF-optimal captured a continuous distribution of FC values via higher spatial resolution (γ), which was offset by a moderate temporal resolution (ω) that kept each region from developing its own network. In NF-optimal, the FPN demonstrated the second highest mean value (t(49)=4.02, p=0.0002) (**Fig. 2E & 2F**), suggesting that in this sector of the parameter-space, the FPN flexibly reorganized across task states more than other networks. NF-standard, however, resulted in an undersized number of networks due to the lower spatial resolution (γ). We reasoned that NF-standard treated the current dataset as unduly discretized.

Network Partition Deviation (NPD)

To reconcile the divergent results and principles of GVC and NF, we created a novel metric termed network partition deviation (NPD). NPD enumerates network reassignments from a pre-defined partition (e.g., the Cole-Anticevic intrinsic partition), across task states. NPD is the percent of task states (e.g., the relative frequency across tasks) in which a given region deviates from a pre-defined partition (**Fig. 2G & 2H**). Of the proposed CCNs, the CON displayed the highest mean NPD (t(10)=4.7, p=0.0008).

Cartography of Cognitive Control Systems

We found that FPN regions expressed high GVC and NF (in an optimized sector of the NF parameter space), yet relatively low NPD. CON regions, however, displayed lower GVC and NF, yet higher NPD. Careful examination of connectivity established by CON and FPN regions clarified this pattern of results. FPN connectivity was globally diverse, whereas CON connectivity was globally uniform (**Fig. 3A**). High GVC requires hub regions – network nodes with extensive connectivity throughout the brain. Thus, the GVC results suggest FPN regions were acting as *flexible hubs*, given their diversity, and CON regions (which have been shown to be hubs as well; see Ito et al., 2017; Power et al., 2013) were acting as *stable hubs*, given their uniformity (**Fig. 3A**). The NPD dissociation between CCNs were mostly attributable to within-network connections being maintained in the FPN but not CON across tasks (**Fig. 3B**). This cartography of network dynamics reveals a dissociation between two prominent CCNs, suggesting parallel distinct mechanisms underlying goal-directed cognition.

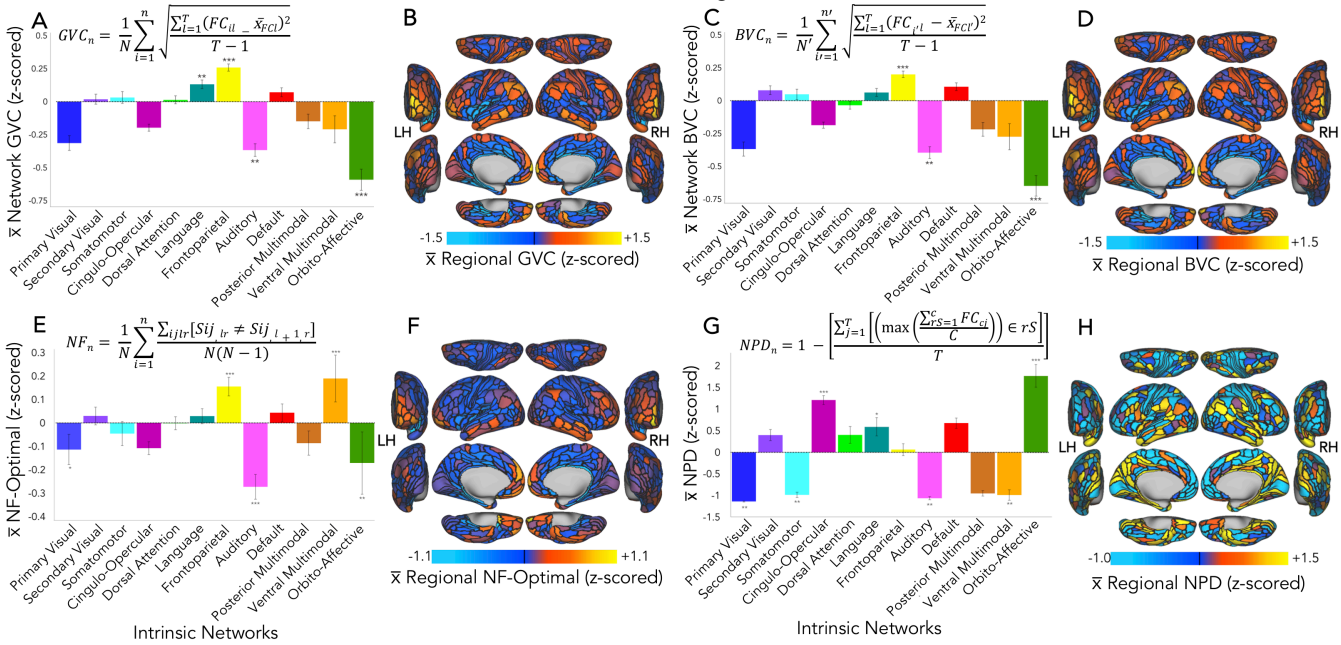

Figure 2: **Cognitive control network metrics. (A)** Network-mean GVC; all means (panels A-H) are across n=50 and C-PRO task states. Networks partitioned as in Fig. 1D. Error bars: standard error of the mean. Asterisks: statistically significant independent-samples t-tests (corrected for false discovery rate, α=0.05). **(B)** Regional mean GVC (same as panel A, but at the region level). **(C)** Network-mean BVC. **(D)** Mean regional BVC. **(E)** Network-mean NF-Optimal. **(F)** Regional mean NF-optimal. **(G)** Network-mean NPD. **(H)** Mean regional NPD. *Formula terms*: n=regions; T=tasks; i=region 1; l=task 1; N=number of regions; FC=adjacency matrix; n'=out-of-network regions; i'=region 1, out-of-network; N'=number of out-of-network regions; $FC_{i'l}$=edge weight, per out-of-network region, per task; FCl'=FC matrix, out-of-network regions only, per task; j=last region; r=last task; γ=spatial resolution; ω=temporal resolution; P=optimization null-model; $Sij_{,l+1,r=}S$, all other tasks; c=network regions; C=number of network regions; rS=pre-defined partition; FC_{cj}=edge weight, per network-region, per task; Q=multi-slice modularity; $\boldsymbol{\delta}$=Kronecker's delta; S=network assignments; $Q = \frac{1}{2\mu}\sum_{ijlr}\{(\mathrm{FCijl}\text{-}\gamma\mathrm{lPijl})\delta\mathrm{lr} + \delta\mathrm{ij}\omega\mathrm{jlr}\}\delta(\mathrm{Sil,\,Sjr})$.

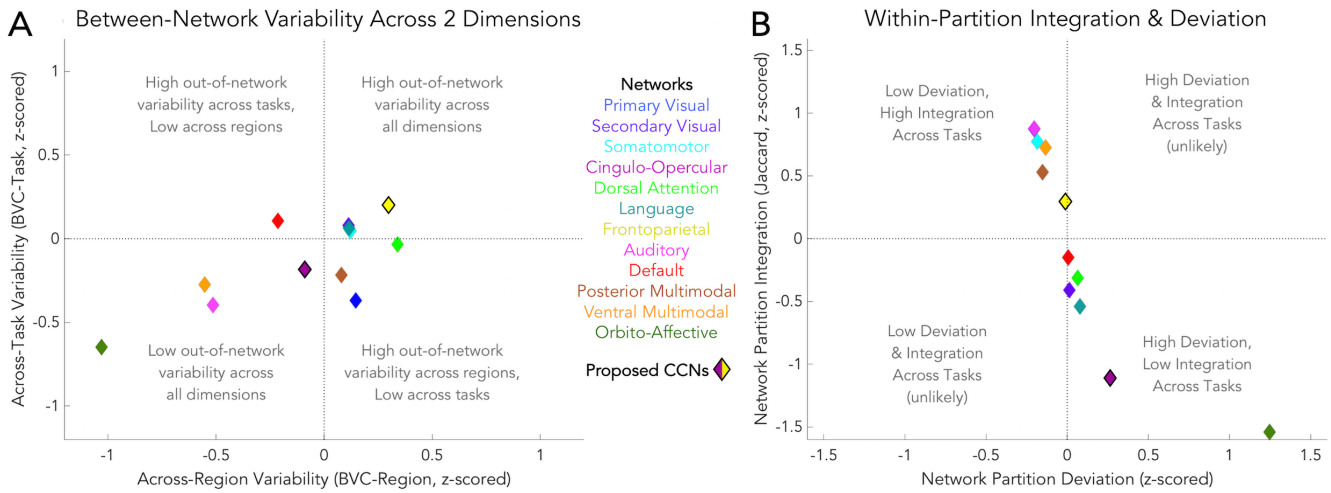

Figure 3: **Cartographies of functional brain systems. (A)** Between-network variability (network means, z-scored) across the task-state dimension (BVC-task; y-axis; as in Fig. 2C) and across the regional dimension (BVC-region; x-axis; as in panel A, except variability measured across regions). CCNs (FPN=yellow, CON=plum) are highlighted with dark black outlines. **(B)** Within-partition integration and deviation (network means, z-scored). Integration (y-axis) is the Jaccard similarity coefficient between task-state reassignments (via NPD) and resting-state assignments (i.e., cross-task partitions versus resting-state partition). Deviation (x-axis) was found as in Fig. 2G.

Acknowledgments

This was supported by the US National Institutes of Health, under awards K99-R00 MH096901 and R01 MH109520, as well as the Rutgers University Behavioral Neuroscience program's graduate assistantship. The content is the sole responsibility of the authors and does not necessarily represent the official views of any of the funding agencies.

References

Bassett, D. S., Wymbs, N.F., Porter, M. A., Mucha, P. J., Carlson, J. M., & Grafton, S.T. (2011). Dynamic reconfiguration of human brain networks during learning. *Proceedings of the National Academy of Sciences of the United States of America*, *108*(18), 7641–7646.

Bassett, D. S., Wymbs, N. F., Rombach, M. P., Porter, M. A., Mucha, P. J., & Grafton, S. T. (2013). Task-based core-periphery organization of human brain dynamics. *PLoS Computational Biology*, *9*(9), e1003171.

Cao, C., Ma, L., & Xu, Y. (2012). Adaptive Control Theory and Applications. *J. Control Science and Engineering*, *2012*.

Chen, M., Kuzmin, K., & Szymanski, B. K. (2015, July 2). *Community Detection via Maximization of Modularity and Its Variants. arXiv [physics.soc-ph]*.

Cole, M. W., Bassett, D. S., Power, J. D., Braver, T. S., & Petersen, S. E. (2014). Intrinsic and task-evoked network architectures of the human brain. *Neuron*, *83*(1), 238–251.

Cole, M. W., Laurent, P., & Stocco, A. (2013). Rapid instructed task learning: a new window into the human brain's unique capacity for flexible cognitive control. *Cognitive, Affective & Behavioral Neuroscience*, *13*(1), 1–22.

Cole, M. W., Reynolds, J. R., Power, J. D., Repovs, G., Anticevic, A., & Braver, T. S. (2013). Multi-task connectivity reveals flexible hubs for adaptive task control. *Nature Neuroscience*, *16*(9), 1348–1355.

Dosenbach, N. U. F., Fair, D. A., Cohen, A. L., Schlaggar, B. L., & Petersen, S. E. (2008). A dual-networks architecture of top-down control. *Trends in Cognitive Sciences*, *12*(3).

Egner, T. (2017). *The Wiley Handbook of Cognitive Control*. John Wiley & Sons.

Glasser, M. F., Coalson, T. S., Robinson, E. C., Hacker, C. D., Harwell, J., Yacoub, E., … Van Essen, D. C. (2016). A multi-modal parcellation of human cerebral cortex. *Nature*, *536*(7615), 171–178.

Guimerà, R., & Amaral, L. A. N. (2005). Cartography of complex networks: modules and universal roles. *Journal of Statistical Mechanics*, *2005*(P02001), nihpa35573.

Hearne, L. J., Cocchi, L., Zalesky, A., & Mattingley, J. B. (2017). Reconfiguration of Brain Network Architectures between Resting-State and Complexity-Dependent Cognitive Reasoning. *The Journal of Neuroscience: The Official Journal of the Society for Neuroscience*, *37*(35).

Ito, T., Kulkarni, K. R., Schultz, D. H., Mill, R. D., Chen, R. H., Solomyak, L. I., & Cole, M. W. (2017). Cognitive task information is transferred between brain regions via resting-state network topology. *Nature Communications*, *8*(1), 1027.

Mattar, M. G., Cole, M. W., Thompson-Schill, S. L., & Bassett, D. S. (2015). A Functional Cartography of Cognitive Systems. *PLoS Computational Biology*, *11*(12), e1004533.

Mill, R. D., Ito, T., & Cole, M. W. (2017). From connectome to cognition: The search for mechanism in human functional brain networks. *NeuroImage*, *160*, 124–139.

Miller, E. K., & Cohen, J. D. (2001). An integrative theory of prefrontal cortex function. *Annual Review of Neuroscience*, *24*.

Mucha, P. J., Richardson, T., Macon, K., Porter, M. A., & Onnela, J.-P. (2010). Community structure in time-dependent, multiscale, and multiplex networks. *Science*, *328*(5980).

Power, J. D., Schlaggar, B. L., Lessov-Schlaggar, C. N., & Petersen, S. E. (2013). Evidence for hubs in human functional brain networks. *Neuron*, *79*(4), 798–813.

Schneider, W. (2003). Controlled & automatic processing: behavior, theory, and biological mechanisms. *Cognitive Science*, *27*(3), 525–559.

Spronk M, Ji JL, Kulkarni K, Repovs G, Anticevic A, Cole MW (Preprint) "Mapping the human brain's cortical-subcortical functional network organization". bioRxiv.